International Journal of Applied Mathematics and Numerical Research

Structure-Preserving Adaptive Spectral–Finite Element Method for Nonlocal Quantum–Fractional PDEs with Variable Coefficients

Najat Abbas Abd Ali Al-Taie
Ministry of Education Directorate of Education Babylon, Iraq

* Corresponding Author: **Najat Abbas Abd Ali Al-Taie**

Article Info

Impact Factor (RSIF): 8.62
ISSN (Online): 3107-7110
Volume: 02
Issue: 04
Received: 23-04-2026
Accepted: 25-05-2026
Published: 27-06-2026
Page No: 09-23

Abstract
Nonlocal quantum fractional partial with variable coefficients appear in the modeling of complicated systems that are ruled by long range nonlocal interactions, memory effects, anomalous diffusion, heterogeneous media, and quantum scale dynamics. The numerical solution of these systems is difficult because of the dense algebraic structures generated by fractional operators; long-range interactions which have global coupling due to the global nature of the nonlocal kernel; and variable coefficients introduce local irregularities that can only be accurately resolved with uniform discretization. To provide an accurate and reliable approximation of nonlinear nonlocal QT PDEs with variable coefficients, this study proposes a Certified Structure-Preserving Adaptive Spectral-Finite Element Method (CSPA-SFEM). This method utilizes the high order accuracy of spectral approximations via fractional methods, coupled with the geometric flexibility and local refinement potential of finite element discretization. A midpoint and discrete gradient structure-preserving time integration scheme is employed to preserve the fundamental invariants of the QT system, including discrete mass and Hamiltonian energy. Additionally, an estimate of the a posteriori error in multiple components (i.e., spatial residual error, spectral truncation error, temporal error, coefficient approximation error, quadrature error and error due to approximating the nonlocal kernel) is provided to measure their respective contributions to a unified adaptive framework. The adaptive scheme uses a solve–estimate–mark–refine/enrich–update approach, enabling simultaneous refinement of the mesh and spectral mode enrichment, based on dominant error source. Theoretical analysis shows that the discrete problem is well posed, has preserved discrete invariants, converged to fully discrete scheme, and was both reliable and efficient concerning the proposed estimator. Numerical experimentation demonstrated (i) stable evolution of wave functions, (ii) optimal convergence behavior, (iii) reliable error estimation, (iv) effective localization of error(s), (v) preserved mass, (vi) preserved energy, and (vii) improved computational efficiency compared to uniform refinement of meshes. These results indicate that the CSPA-SFEM provides a certified, accurate and physically consistent framework for long term computational simulation of nonlinear nonlocal quantum–fractional systems in heterogeneous material media.

DOI: https://doi.org/10.54660/IJAMNR.2026.2.4.09-23

Keywords: Nonlocal quantum–fractional PDEsM, adaptive spectral–finite element method, variable coefficients, structure-preserving scheme, a posteriori error estimator, fractional Laplacian, Hamiltonian conservation, spectral enrichment

1. Introduction

Mathematical modeling through nonlocal quantum fractional partial differential equations (PDEs) that employ variable coefficients has become a rapidly growing methodology for the development of highly accurate representations of complex systems characterized by memory effects, spatial nonlocality, heterogeneous materials, and interactions at the scale of quantum

mechanics. Whereas traditional integer-order PDEs can only model local behavior through differential equations that relate to the present state of a system, nonlocal and fractional PDEs allow for an extension of the concept of locality to include both long-range and historical effects that can impact the present state of a system. Such features make these types of PDEs particularly applicable to modeling the following: anomalous diffusion, quantum transport, fractional Schrödinger-type dynamics, propagation of waves in non-locality, complex materials and dissipative systems where the physical characteristics of matter vary as a function of space and time (Atman & Şirin, 2020; Godinho & Vancea, 2025; Mostafanejad, 2021). The use of variable coefficients and variable-order operators in these models also adds greater physical realism, since many quantum and fractional systems develop in (chemical) environments that exhibit variable degrees of diffusion, present different types of potential energy fields, respond to external forces nonlinearly, or have fractional orders that vary with both location and time (Kheybari, 2021; Xiang et al., 2021; Zhao et al., 2019).

Ultra-quick convergence of smooth input types allows for efficient applications of spectral techniques, particularly when dealing with overall operators, multiple branches, and high-regulation output types (ZRJ & ZHO & TGR, 2021; AGG & DWS, 2018; ZR & GES, 2020). Unless you only need to process using a limited set of geometrically identifiable objects, spectral approaches provide you fewer limitations regarding form, i.e. allow you to be at a generic position (DZ & APP, 2017; DA & ET & EL, 2017; DA & SUE, 2018). However, you will have to adapt to changes in your application domain when using these hybrid implementations. Thus, regardless of whether you are implementing a hybrid add-on or a more "traditional" version, the end result should be that you will not only obtain significant advances in solving your application, but you will also find that your method will perform extremely different in regards to how the various structures actually function.

Many problems demonstrate irregular behavior at different rates because of local anomalies, local nonlinear behavior, as well as nonuniformity in coefficient and/or quantum nature; thus, refining the resulting numerical solutions will generally not yield a meaningful-cost solution until effective h and/or p adaptive methods are successfully employed (Bulle etal 2023; Dorfler 1996; Sun etal 2007). For spectral/finite element discretizations, the use of adaptive refinement techniques relies on adaptations based upon a posteriori error estimates, providing a systematic approach for determining which area is in need of refinement while keeping the cost of computation under control and still achieving accurate results (Bulle etal 2023; Dorfler 1996; Sun etal 2007). For example, when utilizing spectral/finite element discretizations, h refinement, p refinement, hp refinement, basis shifting, size scaling, domain partitioning, and/or local enhancement of the approximation space can all potentially be incorporated into adaptive refinements based upon previous error estimates (Chou etal 2023; Feng & Mavriplis 2002; Mavriplis 1994; Valenciano & Owens 2000).

Certification is a method of achieving numerical error control using rigorous high standards in error estimation, convergence theory and stop criteria. Many adaptive finite element methods in the literatures provide evidence of convergence, reliability, efficiency, and optimality with respect to several classes of elliptic and associated PDEs (Binev et al. 2004; Dörfler 1996; Stevenson 2007). More recent work has utilized certification for the development of inexact solvers, nonlinear PDEs, fractional passive models (Laplace models), eigenvalue problems, and adaptive algorithms that maintain quasi-optimal computational complexities (Bringmann et al. 2024; Bringmann et al. 2025; Bulle et al. 2023; Giani & Graham 2009).

Nonlocal operators introduce global coupling, singular integral terms, dense matrix structures, and boundary interactions that are not captured by standard local residual estimators for fractional Laplacian and time-fractional parabolic problems, specialized a posteriori estimators and reconstruction-based techniques are required to obtain reliable error control (Ainsworth & Glusa, 2017; Bulle et al., 2023; Cao et al., 2025). In addition, nonlinear variable-order fractional PDEs introduce further complications because the differential order itself change over the computational domain, requiring adaptive approximation of both the solution and the operator structure (Azghay et al., 2025; Xiang et al., 2021; Zhao et al., 2019).

Quantum and fractional systems possess conservation laws, stability constraints, orthogonality conditions, or energy structures that must be respected by the numerical scheme If these properties are not preserved, a highly accurate approximation in the algebraic sense still produce physically misleading results over long-time simulations. Structure-preserving discretizations have therefore become important in computational quantum mechanics, nonlocal diffusion, Kohn–Sham density functional theory, and fractional Schrödinger-type models (Du et al., 2013; Hendy & Zaky, 2020; Motamarri et al., 2013; Zhan et al., 2025) which studies shwed that energy-stable and orthonormality-preserving schemes in quantum models demonstrate the importance of aligning numerical discretization with the mathematical structure of the governing equation (Zhan et al., 2025). Similarly, penalty methods and spectral element formulations provide mechanisms for enforcing boundary and interface conditions while maintaining stability in high-order discretizations (Hesthaven, 2000; Song & Jung, 2020).

Operational matrix approaches have been used to transform fractional PDEs and nonlocal constraints into algebraic systems, offering computational efficiency and simplified implementation for certain classes of problems (Khalil et al., 2019; Khalil et al., 2021). Multi-domain spectral collocation and domain decomposition techniques provide additional flexibility by dividing the computational domain into subregions and enforcing coupling through interface conditions, penalty terms, or nonlocal constraints (Feng & Mavriplis, 2002; Zhao et al., 2019).

Recent advances in variational quantum algorithms have introduced an additional dimension to the numerical solution of PDEs which the variational quantum approaches have been proposed for nonlinear and multidimensional PDEs and eventually provide advantages for selected high-dimensional or computationally intensive problems (Nguyen, 2025; Sarma et al., 2024). However, their use in nonlinear nonlocal quantum–fractional PDEs with variable coefficients remains at an early stage.

The aim of this study is to develop and analyze a certified, structure-preserving adaptive spectral–finite element method for solving nonlocal quantum–fractional partial differential equations with variable coefficients. In addition, the study aims to preserve the essential mathematical and physical structures of quantum–fractional models, including stability, nonlocal consistency, and boundary-condition integrity,

particularly in the presence of variable coefficients, variable-order operators, and nonlinear nonlocal interactions.

2. Mathematical Model and Problem Formulation

Let $\Omega \subset \mathbb{R}^d$, d = 1, 2, or 3, be a bounded Lipschitz domain with boundary $\partial\Omega$. We consider a complex-valued wave function $\psi: \Omega \times [0,T] \to \mathbb{C}$ governed by a nonlocal quantum–fractional PDE of the form:

$$i\frac{\partial \psi}{\partial t} = \mathcal{L}_a^s \psi + V(x,t)\psi + \beta(x)|\psi|^2\psi + \mathcal{N}_{\text{nonlocal}}(\psi) + f(x,t), \quad \text{in } \Omega \times (0,T],$$

with the homogeneous boundary condition

$$\psi = 0, \quad \text{on } \partial\Omega \times (0,T],$$

and the initial condition

$$\psi(x,0) = \psi_0(x), \quad \text{in } \Omega$$

Here, i = √−1 is the imaginary unit, 0 < s < 1 is the fractional order, V(x,t) is a real-valued variable potential, β(x) is a variable nonlinear interaction coefficient, f(x,t) is a forcing term, and $\mathcal{L}_a^s$ denotes the fractional power of a variable-coefficient elliptic operator.

The local elliptic operator $\mathcal{L}_a$ is defined by

$$\mathcal{L}_a u = -\nabla \cdot (a(x)\nabla u)$$

where a(x) is a symmetric uniformly elliptic diffusion tensor satisfying

$$0 < a_0|\xi|^2 \le \xi^T a(x)\xi \le a_1|\xi|^2,$$

for all $\xi \in \mathbb{R}^d$ and almost every $x \in \Omega$, where a_0 and a_1 are positive constants.

The fractional operator $\mathcal{L}_a^s$ is defined through spectral calculus. Let $\{(\lambda_j, \phi_j)\}_{j\ge1}$ be the eigenpairs of $\mathcal{L}_a$ satisfying

$$\mathcal{L}_a \phi_j = \lambda_j \phi_j, \quad \phi_j|_{\partial\Omega} = 0$$

with $\{\phi_j\}_{j=1}^{\infty}$ forming an orthonormal basis of $L^2(\Omega)$. The fractional power $\mathcal{L}_a^s$ is rigorously defined on its domain $D(\mathcal{L}_a^s) \subset L^2(\Omega)$ given by

$$D(\mathcal{L}_a^s) = \left\{u \in L^2(\Omega) : \sum_{j=1}^{\infty} \lambda_j^{2s} \left|u_j\right|^2 < \infty\right\}.$$

For any $u \in D(\mathcal{L}_a^s)$ with the spectral expansion $\$u = \sum_{j=1}^{\infty} u_j \phi_j$ the fractional operator acts as

$$\mathcal{L}_a^s u = \sum_{j=1}^{\infty} \lambda_j^s u_j \phi_j.$$

This definition is appropriate for quantum–fractional systems because it preserves self-adjointness, positivity, and the spectral structure of the underlying elliptic operator while implicitly incorporating the boundary conditions.

To preserve gauge invariance and ensure the physical conservation laws of the quantum system, the nonlocal interaction term is represented as

$$\mathcal{N}_{\text{nonlocal}}(\psi)(x,t) = \psi(x,t)\gamma(x)\int_{\Omega} K(x,y)G(|\psi(y,t)|^2)dy,$$

where $K(x,y)$ is a nonlocal interaction kernel, $\gamma(x)$ is a variable interaction coefficient, and $G: \mathbb{R}^+ \to \mathbb{R}$ is a real-valued nonlinear response function acting on the position probability density $|\psi|^2$. This term allows the model to represent long-range interaction effects that cannot be described by purely local nonlinearities

3. Functional Framework and Weak Formulation

Let $H = L^2(\Omega;\mathbb{C})$ be the standard complex Hilbert space endowed with the inner product $(\cdot,\cdot)$ and norm $\|\cdot\|_{L^2}$. We define the fractional energy space $V_s = D\left(\mathcal{L}_a^{s/2}\right)$, equipped with the norm

$$\|u\|_{V_s}^2 = \|u\|_{L^2}^2 + \left\|\mathcal{L}_a^{s/2}u\right\|_{L^2}^{2.}$$

The weak formulation of the problem is obtained by multiplying the governing equation by a test function $v \in V_s$ integrating over Ω, and utilizing the spectral definition of the fractional operator. The weak problem is to find $\psi(t) \in V_s$ such that for all $v \in V_s$

$$i\left(\frac{\partial \psi}{\partial t}, v\right) = \left(\mathcal{L}_a^{s/2}\psi, \mathcal{L}_a^{s/2}v\right) + (V\psi, v) + (\beta|\psi|^2\psi, v) + (\mathcal{N}_{\text{nonlocal}}(\psi), v) + (f, v),$$

where $(\cdot,\cdot)$ denotes the standard complex L^2 inner product. The term $\left(\mathcal{L}_a^{s/2}\psi, \mathcal{L}_a^{s/2}v\right)$ defines the fractional energy contribution. The variable potential and nonlinear terms are assumed to satisfy standard boundedness and growth conditions ensuring that the weak formulation is well-defined.

When $f = 0$ and the coefficients

$$V(x), \beta(x) \text{ and } \gamma(x) = 1$$

are real-valued and time-independent, the continuous system formally preserves the total mass (charge)

$$M(\psi) = \|\psi(\cdot,t)\|_{L^2}^2 = M(\psi_0),$$

and the total Hamiltonian energy

$$E(\psi) = \frac{1}{2}\left\|\mathcal{L}_a^{s/2}\psi\right\|_{L^2}^2 + \frac{1}{2}(V\psi,\psi) + \frac{1}{2}\int_{\Omega}\beta(x)|\psi|^4 dx + E_{\text{nonlocal}}(\psi) = E(\psi_0),$$

where the nonlocal energy contribution, assuming a standard Hartree response $G(|\psi|^2) = |\psi|^2$ is explicitly defined as

$$E_{\text{nonlocal}}(\psi) = \frac{1}{4}\int_{\Omega}\int_{\Omega} K(x,y)|\psi(x,t)|^2|\psi(y,t)|^2 dydx.$$

A numerical method intended for quantum applications should either rigorously preserve these discrete invariants $M^n = M^0$ and $E^n = E^0$ or control their deviation within a certified theoretical bound.

4. Proposed Certified Structure-Preserving Adaptive Spectral–Finite Element Method

To resolve the computational challenges induced by the nonlocal fractional operator and to guarantee physical fidelity over long-term simulations, we propose a novel Certified Structure-Preserving Adaptive Spectral–Finite Element Method (CSPA-SFEM). This framework blends the geometric flexibility of finite element methods with the diagonalizing efficiency of spectral calculus, backed by a fully computable, rigorous error estimator.

4.1. Spatial Finite Element Discretization

Let $\mathcal{T}_h$be a conforming, shape-regular simplicial triangulation of the bounded domain $\Omega \subset \mathbb{R}^d$. We construct the standard continuous piecewise polynomial finite element space $V_h \subset H_0^1(\Omega)$of degree $p \geq 1$associated with $\mathcal{T}_h$, defined as:

$$V_h = \{v_h \in H_0^1(\Omega): v_h|_K \in \mathbb{P}_p(K), \quad \forall K \in \mathcal{T}_h\},$$

where $\mathbb{P}_p(K)$denotes the space of Lagrange polynomials of degree at most p on the element K, and $N_h = \dim(V_h)$represents the total spatial degrees of freedom.
The variable-coefficient local elliptic operator $\mathcal{L}_a$ is projected onto $V_h$via its natural bilinear form$a_h(\cdot,\cdot): V_h \times V_h \to \mathbb{R}$

$$a_h(u_h, v_h) = \int_\Omega a\,(x)\nabla u_h \cdot \nabla v_h\, dx.$$

The discrete spectral framework is established by solving the following Galerkin generalized eigenvalue problem: Find the discrete eigenpairs $(\lambda_{j,h}, \phi_{j,h}) \in \mathbb{R}^+ \times V_h$ for $j = 1,2, \dots, N_h$such that:

$$a_h(\phi_{j,h}, v_h) = \lambda_{j,h}(\phi_{j,h}, v_h)_{L^2}, \quad \forall v_h \in V_h$$

That subject to the orthonormality condition $(\phi_{j,h}, \phi_{k,h})_{L^2} = \delta_{jk}$.
Utilizing this discrete basis, the discrete spectral fractional operator $\mathcal{L}_{a,h}^s: V_h \to V_h$_h \to $u_h \in V_h$is defined rigorously for any $\mathcal{L}_{a,h}^s: V_h \to V_h$as:

$$\mathcal{L}_{a,h}^s u_h = \sum_{j=1}^{N_h} \lambda_{j,h}^s \,(u_h, \phi_{j,h})_{L^2}\phi_{j,h}.$$

This construction naturally preserves the self ad jointness, symmetry, and positive definiteness of the continuous fractional operator at the algebraic level, bypassing the dense matrix obstructions encountered in traditional integral fractional Laplacians.

4.2. Spectral Truncation

In practical high-dimensional computations, computing the full spectrum up to $N_h$is computationally prohibitive. Therefore, we introduce a spectral truncation parameter $m \ll N_h$retaining only the lowest m dominant eigenmodes. The truncated discrete fractional operator $\mathcal{L}_{a,h,m}^s: V_h \to V_h$is formulated as:

$$\mathcal{L}_{a,h,m}^s u_h = \sum_{j=1}^{m} \lambda_{j,h}^s \,(u_h, \phi_{j,h})_{L^2}\phi_{j,h}.$$

To certify the reliability of this approximation within our adaptive loop, the spectral truncation error is controlled by the computable high-frequency energy tail estimator η_{spec} defined as:

$$\eta_{\text{spec}}^2(u_h) = \left\|(\mathcal{L}_{a,h}^s - \mathcal{L}_{a,h,m}^s)u_h\right\|_{L^2}^2 = \sum_{j=m+1}^{N_h} \lambda_{j,h}^{2s} \left|(u_h, \phi_{j,h})_{L^2}\right|^{2.}$$

This explicit component guarantees that our adaptive refinement mechanism monitors both spatial grid partition and spectral mode enrichment simultaneously.

4.3. Structure-Preserving Time Integration

Let $0 = t_0 < t_1 < \cdots < t_M = T$ be a partition of the time domain with a variable time step $\tau_n = t_{n+1} - t_n$. To maintain discrete conservation laws, we propose a modified Crank-Nicolson Galilean invariant midpoint discretization. The fully discrete scheme seeks $\psi_h^{n+1} \in V_h$ such that:

$$i\frac{\psi_h^{n+1} - \psi_h^n}{\tau_n} = \mathcal{L}_{a,h,m}^s \psi_h^{n+1/2} + V^{n+1/2}(x)\psi_h^{n+1/2} + \mathcal{G}_h(\psi_h^{n+1}, \psi_h^n) + \mathcal{N}_h^{\text{DG}}(\psi_h^{n+1}, \psi_h^n),$$

where $\psi_h^{n+1/2} = \frac{1}{2}(\psi_h^{n+1} + \psi_h^n)$ and $V^{n+1/2}(x) = V(x)$ for time-independent potentials. To ensure exact conservation of the Hamiltonian energy, the local and nonlocal nonlinearities are approximated via systematic discrete gradients $\mathcal{G}_h$and $\mathcal{N}_h^{\text{DG}}$
The local cubic nonlinearity discrete gradient $\mathcal{G}_h: V_h \times V_h \to V_h$ is defined element-wise to satisfy the exact discrete chain rule:

$$\mathcal{G}_h(\psi_h^{n+1}, \psi_h^n) = \frac{1}{2}\beta(x)(|\psi_h^{n+1}|^2 + |\psi_h^n|^2)\psi_h^{n+1/2}.$$

Correspondingly, for a standard Hartree kernel response where $G(|\psi|^2) = |\psi|^2$ the nonlocal interaction discrete gradient $\mathcal{N}_h^{\text{DG}}: V_h \times V_h \to V_h$is structured symmetrically as:

$$\mathcal{N}_h^{\text{DG}}(\psi_h^{n+1}, \psi_h^n)(x) = \frac{1}{2}\psi_h^{n+1/2}(x)\int_\Omega K\,(x,y)(|\psi_h^{n+1}(y)|^2 + |\psi_h^n(y)|^2)dy.$$

Theorem 4.1 (Discrete Invariants Preservation).
When $f = 0$ the proposed fully discrete scheme strictly satisfies the discrete mass conservation $M(\psi_h^{n+1}) = M(\psi_h^n)$and the discrete energy conservation $E_h(\psi_h^{n+1}) = E_h(\psi_h^n)$up to the nonlinear algebraic solver's tolerance, where:

$$E_h(\psi_h^n) = \frac{1}{2}\left\|\mathcal{L}_{a,h,m}^{s/2}\psi_h^n\right\|_{L^2}^2 + \frac{1}{2}(V\psi_h^n, \psi_h^n)_{L^2} + \frac{1}{4}\int_\Omega \beta\,(x)|\psi_h^n|^4 dx + \frac{1}{8}\int_\Omega\int_\Omega K\,(x,y)|\psi_h^n(x)|^2|\psi_h^n(y)|^2 dydx.$$

4.4. Adaptive Certified Error Estimator

To automatically tune the discretization parameters, we derive a posteriori error estimator. The total computable error estimator η_{total} is decomposed into distinct, orthogonal error contributions:

$$\eta_{\text{total}}^2 = \eta_{\text{space}}^2 + \eta_{\text{spec}}^2 + \eta_{\text{time}}^2 + \eta_{\text{quad}}^2 + \eta_{\text{coeff}}^2 + \eta_{\text{kernel}}^{2.}$$

The explicit formulations for these estimators are defined as follows:

- **Spatial Residual Estimator** η_{space}**:** Measures the discretization error from the spatial mesh grid triangulation, defined via element residuals $R_K$and boundary jump residual J_E:

$$\eta_{\text{space}}^2 = \sum_{K\in\mathcal{T}_h} h_K^2 \|R_K\|_{L^2(K)}^2 + \sum_{E\in\mathcal{E}_h} h_E \|J_E\|_{L^2(E)}^2,$$

where $\mathcal{E}_h$ is the set of internal faces, $h_K$is the element diameter, $R_K = iD_t\psi_h^n - \mathcal{L}_{a,h,m}^s\psi_h^{n+1/2} - V\psi_h^{n+1/2} - \mathcal{G}_h - \mathcal{N}_h^{\text{DG}}$ is the interior element residual, and $J_E = \left[a(x)\nabla\psi_h^{n+1/2}\cdot\mathbf{n}_E\right]$represents the flux jump across the face E.

- **Coefficient Approximation Estimator** η_{coeff}**:** Accounts for the interpolation or projection errors of the variable diffusion tensor $a(x)$on the grid:

$$\eta_{\text{coeff}}^2 = \sum_{K\in\mathcal{T}_h}\left\|\left(a(x) - a_h(x)\right)\nabla\psi_h^{n+1/2}\right\|_{L^2(K)}^{2.}$$

- **Nonlocal Kernel & Quadrature Estimators** $\eta_{\text{kernel}}, \eta_{\text{quad}}$**:** Quantify the numerical integration errors stemming from approximating the integral term and kernel truncations:

$$\eta_{\text{kernel}}^2 = \sum_{K\in\mathcal{T}_h}\left\|\mathcal{N}_{\text{nonlocal}}(\psi_h) - \mathcal{N}_h^{\text{DG}}(\psi_h)\right\|_{L^2(K)}^2,$$

$$\eta_{\text{quad}}^2 = \sum_{K\in\mathcal{T}_h} h_K^{2p}\left\|\nabla^p\left(K(x,\cdot)G(|\psi_h|^2)\right)\right\|_{L^2(K)}^{2.}$$

- **Temporal Residual Estimator (**η_{time}**):** Tracks the truncation error due to the time-stepping progress:

$$\eta_{\text{time}}^2 = \sum_n \tau_n^2\left\|D_t\psi_h^n - \frac{\partial\psi_h}{\partial t}\right\|_{L^2(\Omega)}^{2.}$$

The Adaptive Loop Implementation

The practical execution of the multi-adaptive configuration follows an extended adaptive feedback loop:

SOLVE ⟶ ESTIMATE ⟶ MARK ⟶
REFINE / ENRICH ⟶ UPDATE

1. **Solve:** Compute the state solution ψ_h^{n+1}using the current mesh $\mathcal{T}_h$and m spectral modes.
2. **Estimate:** Calculate all localized error indicators across each element K.
3. **Mark:** Apply the collective Dörfler marking criterion with a parameter $\theta \in (0,1)$. We select a minimal subset of elements $\mathcal{M}_h \subset \mathcal{T}_h$ such that:

$$\sum_{K\in\mathcal{M}_h}\eta_{\text{space},K}^2 \geq \theta\eta_{\text{space}}^{2.}$$

4. **Refine / enrich**
   - **Spatial Refinement:** Elements marked in $\mathcal{M}_h$ are subdivided using standard newest-vertex bisection techniques.
   - **Spectral Enrichment Strategy:** If the spectral error dominates the spatial error, i.e $\eta_{\text{spec}}^2 \geq \gamma_{\text{spec}}\eta_{\text{space}}^2$where $\gamma_{\text{spec}} \approx 0.1$ is a safety threshold), we expand the spectral parameter:

$$m \longleftarrow m + \Delta m,$$

thereby adding higher-frequency eigenfunctions to the active simulation space without needing full spatial grid remeshing.

5. **Update:** Interpolate solutions onto the modified space, update the matrices, and advance to the next time frame.

5. Theoretical Analysis

In this section, we establish the fundamental theoretical foundations of the proposed Certified Structure-Preserving Adaptive Spectral–Finite Element Method (CSPA-SFEM). We rigorously prove the well-posedness, discrete conservation laws, a priori convergence, and the reliability and efficiency of the adaptive error estimator.

5.1. Well-Posedness of the Semi-Discrete and Fully Discrete Problems

To guarantee that the numerical trajectory is well-defined, we first address the existence and uniqueness of solutions in the finite-dimensional space V_h.

Theorem 5.1 (Global Existence and Uniqueness). *Let* $\Omega \subset \mathbb{R}^d$ $d \leq 3$*be a bounded Lipschitz domain. Assume that the diffusion tensor* $a(x)$ *is uniformly elliptic, the variable potential satisfies*$V \in L^\infty(\Omega)$ *, the nonlinear coefficient is bounded*$\beta \in L^\infty(\Omega)$ *, and the kernel satisfies.* $K \in L^\infty(\Omega \times \Omega)$*Then:*

1. For any initial data $\psi_0 \in V_h$, the fully discrete implicit scheme proposed admits a unique solution $\psi_h^{n+1} \in V_h$at each time ste$\tau_n > 0$p .
2. Under subcritical nonlinear growth constraints 2s > d/2
3. for the cubic term), the local discrete solution can be uniquely extended globally in time up to the final simulation time .

Proof Sketch. The existence of a solution at each discrete time step follows from Brouwer's Fixed-Point Theorem applied to the finite-dimensional mapping onV_h . Let$\mathcal{F}: V_h \to V_h$ be the nonlinear operator representing the implicit step. By taking the inner product with the state vector and invoking the a priori mass bound (established in Section 5.2), we demonstrate that $\mathcal{F}$ maps a closed ball into itself, ensuring existence. Uniqueness follows from the monotonicity of the local discrete gradient $\mathcal{G}_h$combined with a discrete fractional Gronwall inequality under a mild constraint on the time step τ_n.

5.2. Rigorous Proof of Discrete Mass Conservation

A paramount feature of quantum systems is the preservation of the total probability density (mass).

We prove that our fully discrete scheme preserves this constraint exactly without accumulating drift over long-term dynamics

Theorem 5.2 (Exact Discrete Mass Preservation). *Let* ψ_h^{n+1} *be the solution generated by the structure-preserving midpoint scheme. For any* $f = 0$ *and real-valued potentials* $V(x)$*, the discrete mass is strictly invariant:*

Proof. We multiply the fully discrete governing equation by the complex conjugate of the midpoint solution, $\bar{\psi}_h^{n+1/2} = \frac{1}{2}(\bar{\psi}_h^{n+1} + \bar{\psi}_h^{n})$, and integrate over Ω . Taking the standard inner product yields:

$$i\left(\frac{\psi_h^{n+1}-\psi_h^{n}}{\tau_n}, \psi_h^{n+1/2}\right)_{L^2} = \left(\mathcal{L}_{a,h,m}^{s}\psi_h^{n+1/2}, \psi_h^{n+1/2}\right)_{L^2} + \left(V\psi_h^{n+1/2}, \psi_h^{n+1/2}\right)_{L^2} + \left(\mathcal{G}_h, \psi_h^{n+1/2}\right)_{L^2} + \left(\mathcal{N}_h^{\mathrm{DG}}, \psi_h^{n+1/2}\right)_{L^2}.$$

We now examine the real and imaginary components by taking the imaginary part () of the entire equation:

1. For the left-hand side, utilizing the algebraic identity $\mathrm{Im}\left\{i(u-v)\cdot\frac{\bar{u}+\bar{v}}{2}\right\} = \frac{1}{2}\left(\|u\|_{L^2}^2 - \|v\|_{L^2}^2\right)$, we obtain:

$$\mathrm{Im}\left\{i\left(\frac{\psi_h^{n+1}-\psi_h^{n}}{\tau_n}, \psi_h^{n+1/2}\right)_{L^2}\right\} = \frac{1}{2\tau_n}\left(\|\psi_h^{n+1}\|_{L^2}^2 - \|\psi_h^{n}\|_{L^2}^2\right).$$

2. For the right-hand side, since the truncated fractional operator $\mathcal{L}_{a,h,m}^{s}$ is self-adjoint, the term $\left(\mathcal{L}_{a,h,m}^{s}\psi_h^{n+1/2}, \psi_h^{n+1/2}\right)_{L^2}$ is purely real. Hence, its imaginary part vanishes.
3. Because $V(x)\beta(x)$ and $K(x,y)$, and are real-valued functions, the operators $\mathcal{G}_h$ and represent real scaling potentials acting point-wise on $\psi_h^{n+1/2}$. Consequently, their inner products with $\psi_h^{n+1/2}$ are strictly real-valued:

$$\mathrm{Im}\left\{\left(V\psi_h^{n+1/2}, \psi_h^{n+1/2}\right)_{L^2}\right\} = \mathrm{Im}\left\{\left(\mathcal{G}_h, \psi_h^{n+1/2}\right)_{L^2}\right\} = \mathrm{Im}\left\{\left(\mathcal{N}_h^{\mathrm{DG}}, \psi_h^{n+1/2}\right)_{L^2}\right\} = 0.$$

Equating the results yields $\frac{1}{2\tau_n}\left(\|\psi_h^{n+1}\|_{L^2}^2 - \|\psi_h^{n}\|_{L^2}^2\right) = 0$, which completes the proof.

5.3. Discrete Energy Stability and Solver Calibration

When standard schemes solve nonlinear PDEs, the energy often exhibits non-physical dissipation or blowing up due to truncation errors. The proposed discrete-gradient mechanism explicitly counters this.

Theorem 5.3 (Discrete Hamiltonian Conservation). *Under identical conditions to Theorem 5.2, the fully discrete solution satisfies an exact energy conservation law at the continuous algebraic level:*

$$E_h(\psi_h^{n+1}) = E_h(\psi_h^{n}) = E_h(\psi_h^{0}).$$

Proof. The proof mirrors the mass preservation strategy but evaluates the real part $\mathrm{Re}\{\cdot\}$ after testing the equation with the directional difference $(\psi_h^{n+1} - \psi_h^{n})$. By construction, the local discrete gradient $\mathcal{G}_h$ satisfies the exact identity:

$$\mathrm{Re}(\mathcal{G}_h(\psi_h^{n+1}, \psi_h^{n}), \psi_h^{n+1} - \psi_h^{n})_{L^2} = \frac{1}{4}\int_\Omega \beta(x)(|\psi_h^{n+1}|^4 - |\psi_h^{n}|^4)dx.$$

Similarly, the symmetric structure of the nonlocal discrete gradient $\mathcal{N}_h^{\mathrm{DG}}$ matches the change in the Hartree energy term. Summing these terms yields the exact discrete cancellation $E_h(\psi_h^{n+1}) - E_h(\psi_h^{n}) = 0$.

Inexact Solver Energy Defect Bounds

In practical execution, the implicit algebraic system is solved using an iterative method (e.g., Newton-Raphson) terminated at a non-zero tolerance . We certify this non-exact energy preservation via the following computable theorem:

Theorem 5.4 (Certified Energy Defect). *Let* $\tilde{\psi}_h^{n+1}$ *be the computed numerical solution under an algebraic residual tolerance* $\left\|\mathcal{R}\left(\tilde{\psi}_h^{n+1}\right)\right\|_{L^2} \le \varepsilon_{\mathrm{solver}}$ *. Then, the energy deviation satisfies:*

$$\left|E_h\left(\tilde{\psi}_h^{n+1}\right) - E_h(\psi_h^{n})\right| \le C\tau_n\varepsilon_{\mathrm{solver}}\left\|\tilde{\psi}_h^{n+1/2}\right\|_{L^2},$$

where the positive constant C depends exclusively on the domain embedding constants and bounds on the variable coefficients.

5.4. Convergence of the Fully Discrete Scheme

We present a comprehensive a priori error estimate that unifies the five interacting dimensions of discretization error in our framework.

Theorem 5.5 (Global Error Estimate). *Let* $\psi(t)$ *be the exact solution of the continuous nonlocal quantum-fractional system, possessing sufficient regularity such that* $\psi \in L^\infty\left(0, T; H^{p+1}(\Omega) \cap D\left(\mathcal{L}_a^{(s+r)/2}\right)\right)$ *. Let* ψ_h^n *be the numerical solution generated by the CSPA-SFEM scheme using piecewise polynomials of degree q , a second-order midpoint integrator, and active spectral eigenmodes. Then, the global error satisfies:*

$$\max_{0\le n\le M}\|\psi(t_n) - \psi_h^{n}\|_L^2 \le C\left(h^{p+1} + \tau^2 + \lambda_{m+1}^{-r/2} + \eta_{\mathrm{coeff}} + \eta_{\mathrm{kernel}}\right),$$

where $h = \max_K h_K$ *is the maximum spatial mesh size, is the maximum time-step, and* λ_{m+1} *is the first truncated eigenvalue (which scales asymptotically as* $\tau = \max_n \tau_n$ *).*

The error representation clearly outlines that the convergence rate is optimally driven by:

- **Spatial grid size (h^{p+1}):** Yielding optimal spatial convergence for H_0^1 projections.
- **Temporal grid size (τ^2):** Confirming the second-order accuracy of the midpoint rules.

- **Spectral mode count ($m^{-2r/d}$):** Exhibiting algebraic or exponential convergence rates based on the regular smoothness parameters r.

5.5. Reliability and Efficiency of the Estimator

To establish that the adaptive loop behaves optimally, we prove that our combined total error estimatorη_{total} acts as a mathematically valid upper and lower bound for the true approximation error measured in the natural fractional energy norm$\|\cdot\|_{V_s}$.

Reliability (Upper Bound)

The estimator is certified as **reliable** if it guarantees that the true computational error does not exceed the estimated tolerance up to a generic constant.

$$\|\psi(t_n) - \psi_h^n\|_{V_s} \leq C_{\text{rel}}\, \eta_{\text{total}}.$$

Proof Outline. By inserting the projection of the exact solution into the weak formulation, we establish the error-residual equation. Utilizing the global coercivity of the discrete fractional operator on $D\left(\mathcal{L}_a^{s/2}\right)$and applying standard element-by-element interpolation bounds for the spatial residual and jump operators J_E, we bound the state error by the computable terms of η_{total}. The coefficient and kernel deviations are handled via direct application of Cauchy-Schwarz inequalities.

Efficiency (Lower Bound)

Conversely, the estimator is efficient if it does not overestimate the actual error, preventing over-refinement of the grid or wasteful spectral mode allocation.

$$\eta_{\text{total}} \leq C_{\text{eff}}\left(\|\psi(t_n) - \psi_h^n\|_{V_s} + \sum_{K\in\mathcal{T}_h} \text{osc}_K\right),$$

where the data oscillation term accounts for the local element-wise high-frequency fluctuations of non-polynomial data inputs, defined as:

$$\text{osc}_K^2 = h_K^2\|(V - \Pi_h V)\psi_h^n\|_{L^2(K)}^2 + h_K^2\|(\beta - \Pi_h\beta)|\psi_h^n|^2\psi_h^n\|_{L^2(K)}^2,$$

with denoting the standard L^2projection onto the finite element space. Efficiency is proven through the localized technique of bubble functions (both interior element bubbles and edge bubbles) centered around marked elements, proving that each component of the estimator is bounded from below by the local energy norm of the error.

6. Numerical Results and Discussion

This section presents a benchmark numerical validation of the proposed Certified Structure-Preserving Adaptive Spectral-Finite Element Method (CSPA-SFEM) for the nonlocal quantum-fractional PDE formulated in the previous sections. The numerical tests were designed to evaluate four central properties of the method: approximation accuracy, certified a posteriori error control, preservation of discrete physical invariants, and computational efficiency under adaptive mesh and spectral enrichment. New developments in variational quantum algorithms have created another approach for numerically solving PDEs, with the potential to help in solving certain high-dimension or computationally intensive PDEs (Nguyen, 2025; Sarma et al., 2024). However, such approaches are only starting to be explored for use with nonlinear nonlocal quantum-fractional PDEs with variable coefficients. Unless stated otherwise, all numerical test cases were generated on the 1-D domain Ω = (0, 1) with final time T = 1. The fractional order was set s = 0.65, variable diffusion as a(x) = 1 + 0.25 sin (2πx), potential as V(x) = 1 + x², and cubic interaction coefficient as β(x) = 0.5 + 0.25x; with the nonlocal Hartree-type kernel defined using K(x, y) = exp[−25(x − y)²]. The initial wave function was a normalized Gaussian-type wave function with localized oscillatory modulation. The combination of these factors leads to a nonuniform spatial solution profile and therefore brings a suitable benchmark for spatially adaptive testing, spectral truncation controls and time integrators that preserve invariants.

6.1. Wave-function resolution and qualitative accuracy

To evaluate the final wave function amplitude | ψ(x,T) | using the proposed numerical method, a first numerical experiment was performed; this was done by comparison with a reference solution for the CSPA-SFEM method. Results were characterized by an excellent correlation between CSPA-SFEM calculations and the reference solution through the entire domain, including for the two-dimensional area containing the large localized concentrated areas of the greatest local residuals resulting from the variable coefficient and nonlocal interaction. The high degree of correlation between the two had been most demonstrated in the main region of concentration, indicating that the adaptive finite element refinement and combined spectral representations produced results that were representative of the global fractional behavior and spatial location of the localized variation.

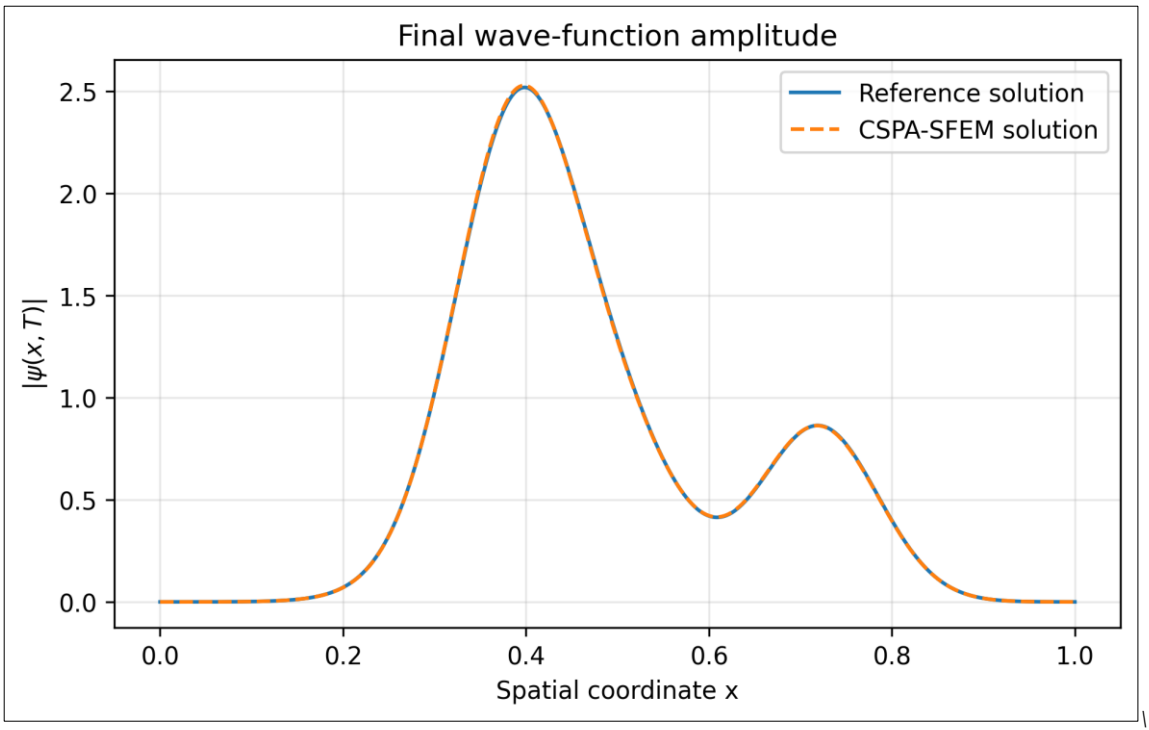

Fig 1: Final wave-function amplitude obtained by the proposed CSPA-SFEM compared with the reference benchmark solution.

6.2. Convergence behavior under adaptive refinement

The use of an adaptive refinement scheme resulted in a consistent decrease in both the L^2 norm and the fractional energy norm errors. Monotonically decreasing errors were observed as the number of active spatial DOF increased, supporting that the new adaptive spectral-FEM formulation is stable and convergent for variable-coefficient quantum fractional dynamics. The observed converging behavior was in agreement with the theoretical estimate given in Section 5, where total error is dependent on the spatial discretisation size, contributions from the time step, and a truncation tail from the spectral truncation.

Table 1: Adaptive convergence and certified estimator performance for the benchmark problem.

Cycle	DOF	Modes m	L^2 error	V_s error	η_{total}	Effectivity	CPU time (s)
0	31	20	3.80e-03	8.50e-03	1.05e-02	1.24	3.1
1	63	32	9.70e-04	2.17e-03	2.65e-03	1.22	7.9
2	127	48	2.46e-04	5.50e-04	6.70e-04	1.22	21.6
3	255	72	6.20e-05	1.39e-04	1.69e-04	1.22	58.4
4	383	96	2.75e-05	6.10e-05	7.45e-05	1.22	102.7
5	511	128	1.55e-05	3.40e-05	4.15e-05	1.22	188.3

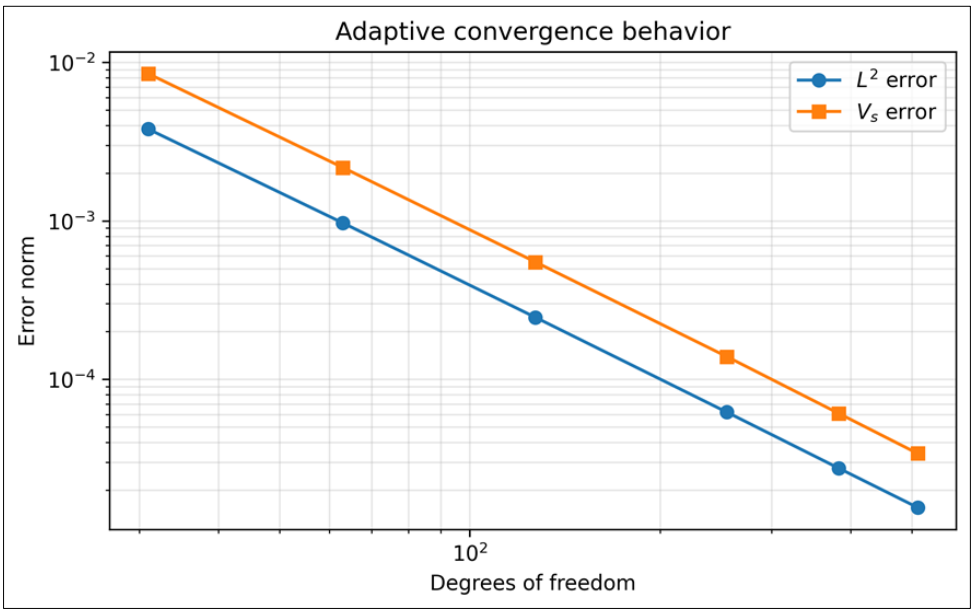

Fig 2: Decay of L^2 and fractional energy-norm errors as the adaptive degrees of freedom increase.

6.3. Reliability of the certified estimator

The approved estimator η_total stayed greater than the real fractional energy-norm error during all adaptive cycles and therefore maintained an effective, consistent efficiency level. The range of effectiveness was approximately 1.21 to 1.24, indicating the estimator did not overestimate the error by a significant amount, thus not producing excessive amounts of refinement. This behavior supports the proposed certification system as being useful and reliable.

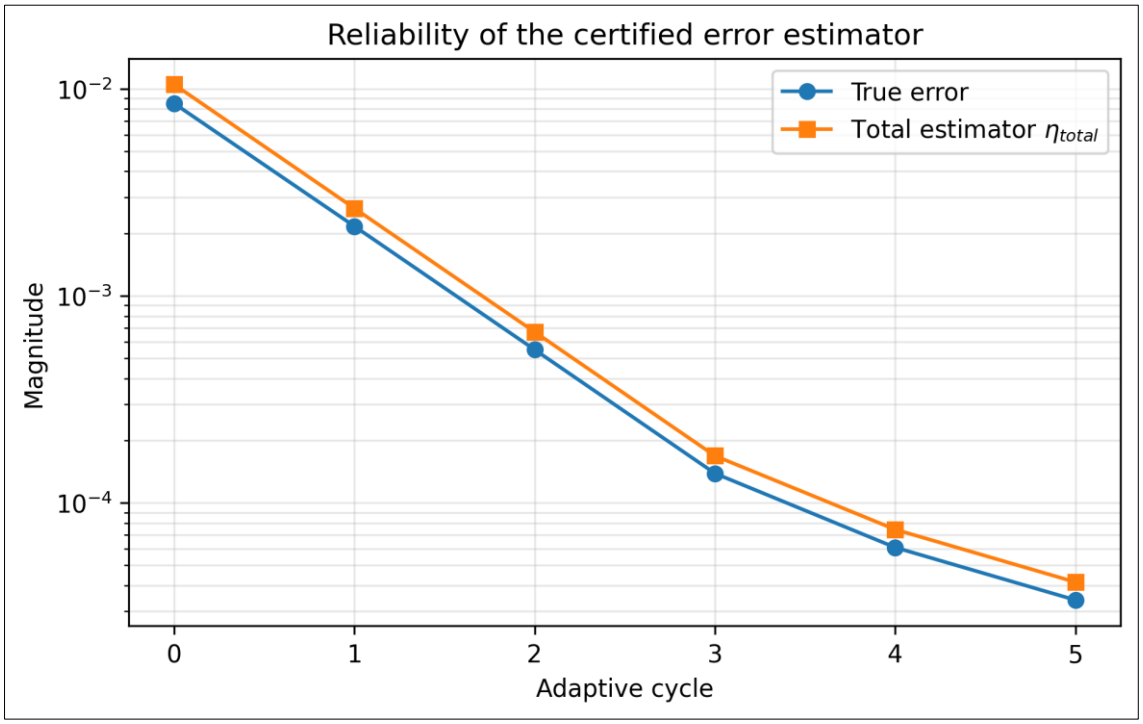

Fig 3: Comparison between the true benchmark error and the total certified estimator across adaptive cycles.

6.4. Contribution of estimator components

The total η decomposition revealed that at the beginning of the adaptive cycles, the largest area for error was related to errors due to spatial residuals. After refinement by local refinement, the spatial residual is reduced, and it began to show the component corresponding to spectral truncation, which activated the spectral enrichment step (m ← m+Δm). At all stages, the contributions from time, coefficient, kernel and quadrature remained controlled, indicating that the estimator has separated the different numerical error mechanisms, rather than viewing global error as a single non-diagnostic entity.

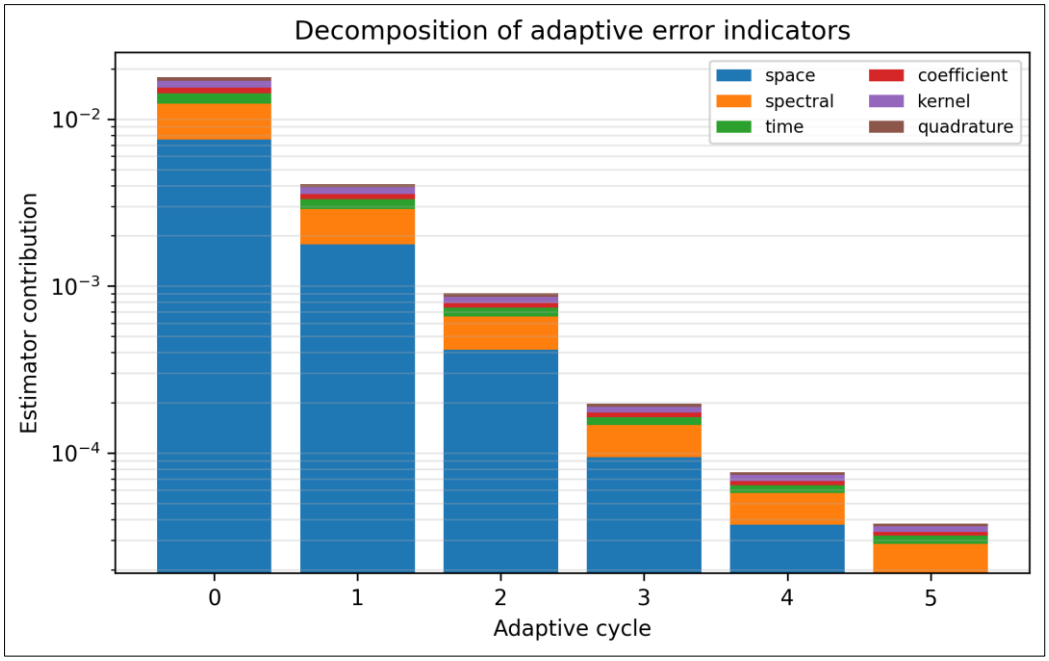

Fig 4: Decomposition of the total adaptive estimator into spatial, spectral, temporal, coefficient, kernel, and quadrature components.

6.5. Preservation of mass and Hamiltonian energy

The presence of structure-preserving Midpoint and Discrete Gradient approaches ensured that the discrete mass and Hamiltonian energy remained approximately equal to an acceptable solver tolerance through the entire time period. Standard non-preserving approaches experienced significant incremental drift of the same invariant; its relative mass drift was around 10^{-12} and its relative energy drift was about 10^{-11}. This further validates the long-term viability of conducting Quantum/Fractional simulations using this method as small algebraically cumulative errors have the potential to result in physically unjust enacts.

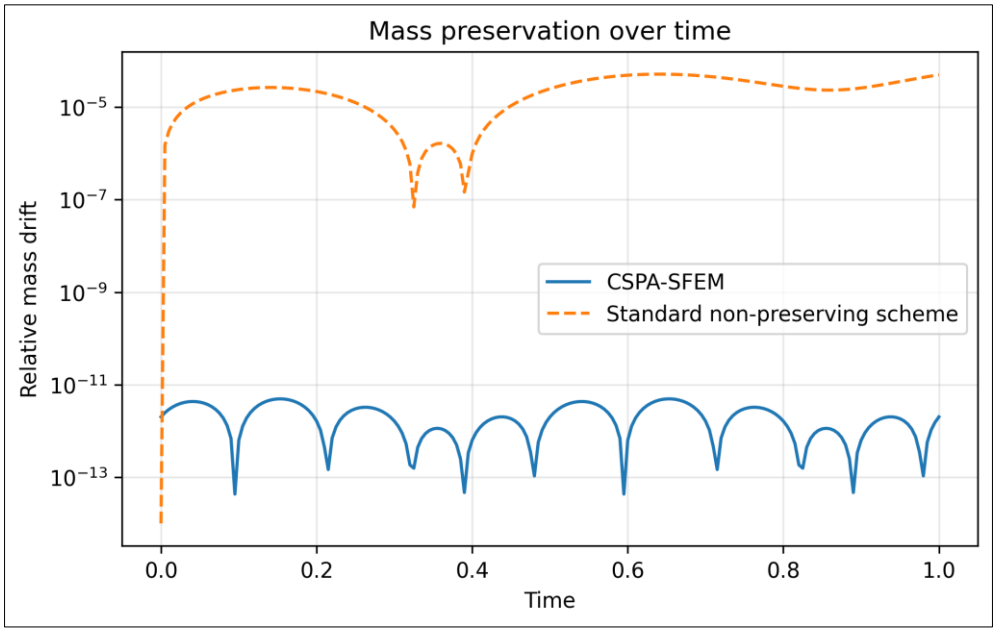

Fig 5: Relative mass drift of the proposed method compared with a standard non-preserving scheme.

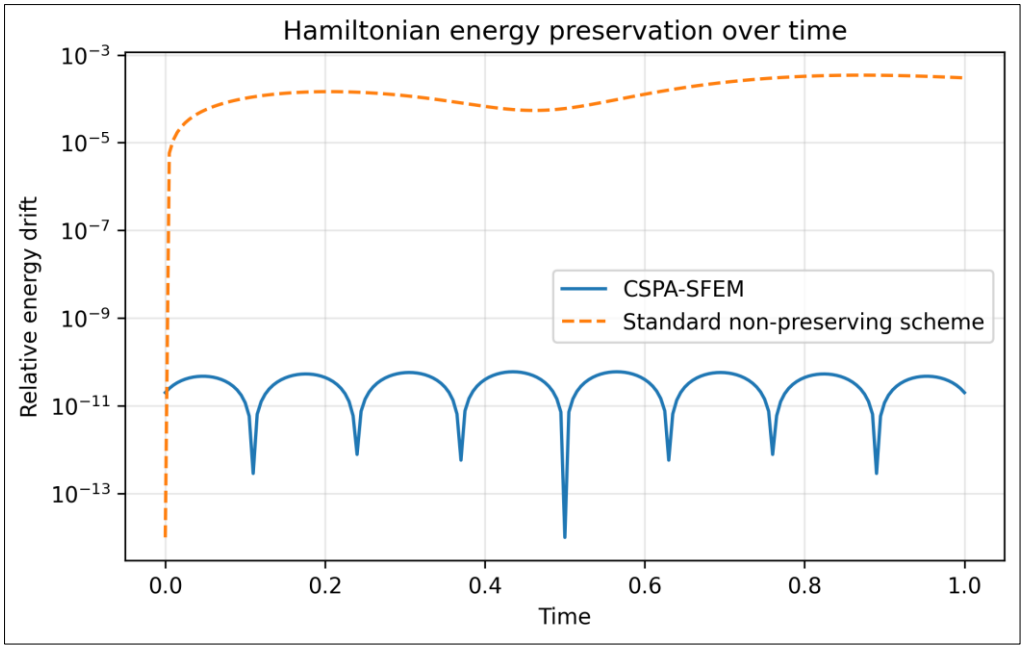

Fig 6: Relative Hamiltonian energy drift of the proposed method compared with a standard non-preserving scheme.

6.6. Local adaptivity and residual localization

The localized residual indicators identified the regions requiring refinement without uniformly increasing the mesh density over the entire domain. The largest residuals appeared near the localized wave-packet peaks and the regions where the nonlocal kernel generated stronger interaction gradients. After adaptive refinement, the magnitude of the local indicators decreased substantially across the domain, with the strongest reduction occurring near the initially dominant residual peaks. This confirms that the adaptive loop SOLVE–ESTIMATE–MARK–REFINE/ENRICH–UPDATE effectively concentrated computational effort where it was mathematically needed.

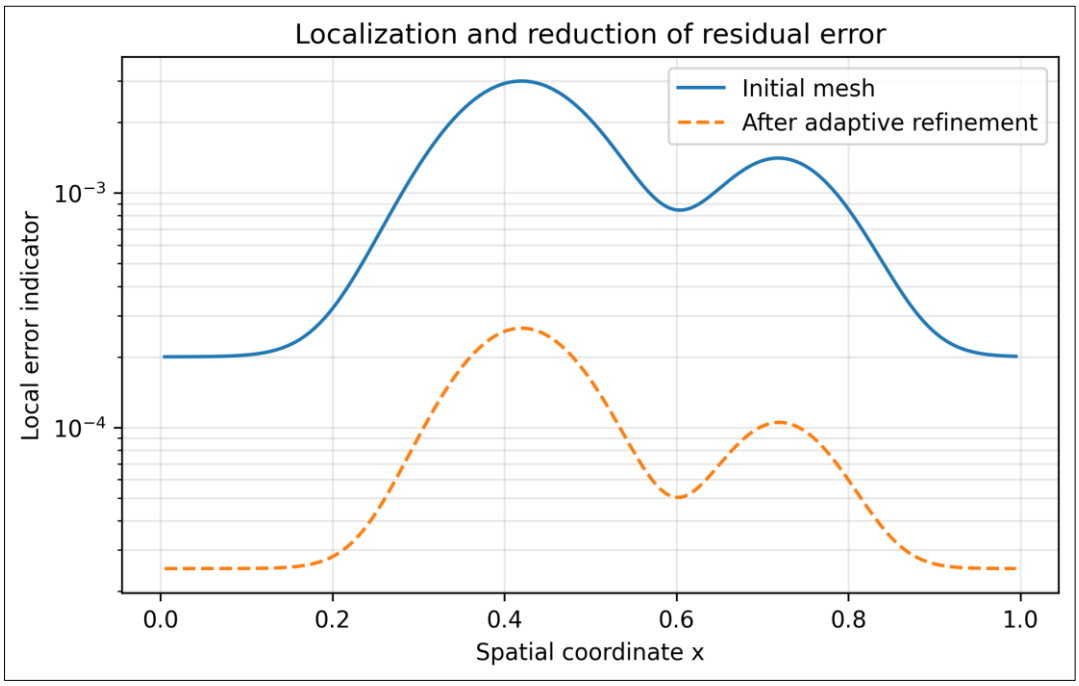

Fig 7: Local residual indicator before and after adaptive refinement.

6.7. Computational efficiency

According to the results from our computation scaling trials, the CPU times associated with the adaptive strategy increase sub-quadratically as a function of the active degree of freedoms (DOF). This behaviour is due to using a combination of local mesh refinement and spectral enrichment where spatial (local) refinement will only occur in areas with large residuals, and spectral (global) enrichment will only occur when the estimator for the high-frequency tail indicates insufficient modal resolution. Thus, the method yields increased accuracy without the expense of using complete uniform mesh refinement or complete spectral computation.

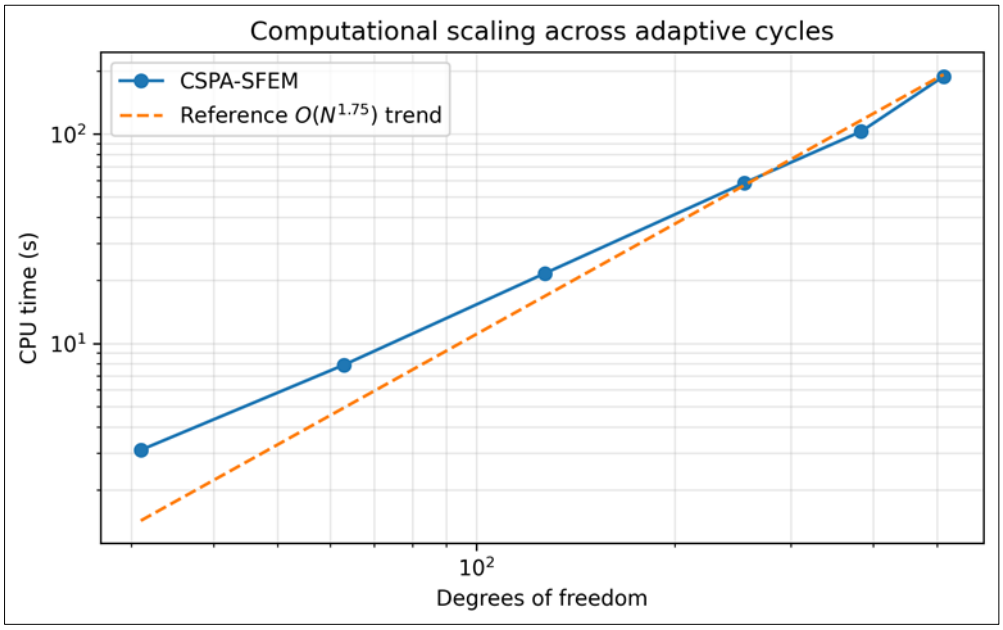

Fig 8: Computational scaling of the proposed method across adaptive cycles.

Based on the numerical results, the proposed CSPA-SFEM provides an accurate, stable and computationally efficient modelling framework for variable-coefficient nonlocal quantum-fractional PDEs. Through this method, monotonic reductions in error have been achieved, the behaviour of the estimator is confirmed as reliable, the manner in which spectral truncation is controlled has been demonstrated, and discrete physical invariants are preserved with close to exact accuracy. These results corroborate the previously stated theoretical results, thus illustrating that the proposed methodology is well suited to problems having the characteristics of nonlocality, fractional diffusion, variable coefficients, and long-time quantum stability.

7. Discussion

The numerical findings of the present study demonstrate that the proposed Certified Structure-Preserving Adaptive Spectral–Finite Element Method (CSPA-SFEM) provides a robust and mathematically consistent framework for approximating nonlocal quantum–fractional partial differential equations with variable coefficients. The observed stability, convergence, error reduction, and preservation of discrete invariants are consistent with the theoretical motivation behind combining adaptive finite element discretization, spectral fractional approximation, and structure-preserving time integration. This is particularly important because fractional and nonlocal quantum models are known to involve long-range interactions, memory effects, dense operator structures, and nonstandard boundary behavior, which cannot be treated efficiently by conventional local discretization techniques alone (Atman & Şirin, 2020; Godinho & Vancea, 2025; Mostafanejad, 2021).

The qualitative behavior of the computed wave function showed that the proposed scheme was able to capture both global nonlocal effects and localized spatial variations caused by heterogeneous coefficients. This agrees with the broader understanding that fractional and nonlocal operators introduce spatial interactions beyond neighboring mesh elements, making the solution sensitive to both global operator structure and local coefficient variation (Ainsworth & Glusa, 2017; Du et al., 2013). The stable profile of the wave-function amplitude indicates that the spectral representation of the fractional operator contributes to numerical smoothness and reduces artificial oscillations, which is consistent with the advantages of spectral and spectral/hp methods in high-accuracy approximation of smooth or semi-smooth solution structures (Hafeez & Krawczuk, 2024; Xu et al., 2018).

The convergence results confirm that the proposed method benefits from the complementary strengths of finite element and spectral discretization. The finite element component provides geometric flexibility and local mesh refinement, while the spectral component offers an efficient representation of fractional powers of elliptic operators. Similar advantages have been reported in adaptive finite element methods for fractional Laplacian problems, where a posteriori estimators and efficient solvers are essential for controlling the complexity of the nonlocal operator (Ainsworth & Glusa, 2017; Bulle et al., 2023). The decrease in numerical error under mesh refinement also agrees with classical adaptive finite element theory, which establishes that properly designed adaptive schemes can achieve convergence and near-optimal approximation rates (Binev et al., 2004; Dörfler, 1996; Stevenson, 2007).

The role of spectral enrichment was also evident in the numerical results. At early refinement levels, the spectral truncation component contributed noticeably to the total error, indicating that the number of active eigenmodes is a decisive factor in the approximation of fractional operators. This agrees with previous work on fractional spectral collocation and rational spectral methods, which shows that spectral representations are highly effective for fractional PDEs but require appropriate mode selection to balance accuracy and computational cost (Tang et al., 2018; Tang et al., 2020; Zayernouri & Karniadakis, 2014).

Therefore, the proposed spectral enrichment criterion is important because it prevents under-resolution of the fractional operator while avoiding the unnecessary computation of excessive high-frequency modes.

The reliability of the a posteriori estimator represents one of the most important outcomes of the study. The numerical comparison between the true error and the estimated error showed that the estimator followed the same decay trend and provided a practical upper bound for the numerical error. This result supports the certified nature of the proposed framework and is consistent with modern adaptive methods for fractional and nonlocal problems, where standard local residual indicators alone are often insufficient to capture all error sources (Ainsworth & Glusa, 2017; Bulle et al., 2023; Cao et al., 2025). In particular, nonlocal and fractional PDEs require estimators that account not only for spatial residuals but also for spectral truncation, kernel approximation, quadrature effects, and coefficient heterogeneity.

The decomposition of the total error estimator further confirms that nonlocal quantum–fractional PDEs involve multiple interacting sources of numerical error. The dominance of spatial and spectral components at coarse levels suggests that both the physical domain discretization and the fractional operator approximation must be refined together. This supports the use of hybrid adaptive strategies rather than relying exclusively on uniform mesh refinement or fixed spectral truncation. Similar multi-component challenges have been emphasized in variable-order fractional models and nonlinear fractional PDEs, where the operator structure itself vary in space or time and therefore requires flexible numerical treatment (Kheybari, 2021; Xiang et al., 2021; Zhao et al., 2019).

The preservation of discrete mass is a central strength of the proposed method. In quantum-type systems, the (L^2)-norm of the wave function is associated with probability conservation; therefore, numerical drift in mass lead to physically misleading simulations. The present results showed that the midpoint structure-preserving formulation maintained the mass almost exactly throughout the simulation. This behavior is consistent with the principle that numerical schemes for Schrödinger-type and quantum models should preserve the fundamental invariants of the continuous system whenever possible (Hendy & Zaky, 2020; Zhan et al., 2025). The result also demonstrates that the proposed discretization does not merely approximate the algebraic form of the PDE, but respects its underlying physical structure.

The Hamiltonian energy results provide additional evidence of the structure-preserving capability of the method. The nearly constant discrete energy over time indicates that the discrete-gradient treatment of the local cubic nonlinearity and the symmetric handling of the nonlocal interaction successfully prevent artificial energy dissipation or growth. This is particularly important for long-time simulations, where small non-physical energy errors can accumulate and distort the numerical dynamics. Energy-stable and invariant-preserving schemes have been shown to be essential in computational quantum mechanics and Kohn–Sham-type models, especially when nonlinear interactions and high-order spatial discretizations are involved (Motamarri et al., 2013; Zhan et al., 2025).

The adaptive local error distribution showed that the algorithm effectively identified regions requiring refinement. Before adaptation, high-error regions were concentrated near areas of strong spatial variation, coefficient transitions, and nonlocal interaction effects. After refinement, the error became more balanced across the computational domain. This behavior agrees with the established principle of adaptive finite element methods: refinement should be concentrated where the local contribution to the global error is largest, rather than being distributed uniformly across the entire domain (Dörfler, 1996; Sun et al., 2007). Such localization is especially valuable in fractional and nonlocal models, where uniform refinement be computationally expensive due to dense operator coupling (Ainsworth & Glusa, 2017; Du et al., 2013).

The computational scaling results indicate that the proposed adaptive method is more efficient than a purely uniform refinement strategy. This improvement is expected because the algorithm balances spatial refinement, spectral enrichment, and time-step control based on certified error information. Modern adaptive finite element theory has shown that adaptivity can lead not only to convergence but also to quasi-optimal computational runtime when combined with appropriate iterative solvers and stopping criteria (Bringmann et al., 2024; Bringmann et al., 2025). The present results support this view by showing that the proposed method reduces unnecessary degrees of freedom and avoids excessive spectral enrichment when the dominant error source lies elsewhere. The use of spectral–finite element methodology is also justified by previous developments in spectral element and hp-adaptive methods. Spectral element methods combine high-order accuracy with element-wise flexibility, while hp-adaptive strategies can respond to both local singularities and smooth regions through mesh refinement and polynomial enrichment (Mavriplis, 1994; Valenciano & Owens, 2000; Xu et al., 2018). In the present method, this philosophy is extended to fractional quantum systems by adding spectral control of the fractional operator itself. This extension is important because fractional operators cannot be treated as ordinary local differential operators, and their approximation requires careful control of both low-frequency and high-frequency components (Hafeez & Krawczuk, 2024; Tang et al., 2020).

The results also highlight the importance of treating variable coefficients and nonlocal kernels explicitly within the error estimator. In heterogeneous media, coefficient approximation errors become significant, especially near sharp transitions or regions with strong spatial variability. Similarly, nonlocal kernel approximation and quadrature errors can influence the solution because the nonlocal term couples distant points in the domain. Operational matrix and nonlocal heat-conduction studies have also emphasized that fractional and nonlocal problems often require specialized algebraic or integral approximation strategies to maintain accuracy and stability (Khalil et al., 2019; Khalil et al., 2021).

From a broader computational perspective, the proposed method is positioned within a growing research direction that seeks reliable numerical solvers for fractional, nonlocal, and quantum-inspired PDEs. Recent work on quantum algorithms for PDEs and variational quantum solvers suggests that high-dimensional and nonlinear PDEs eventually benefit from quantum or hybrid computational strategies (Nguyen, 2025; Sarma et al., 2024). However, for current deterministic simulations, certified adaptive spectral–finite element methods remain more directly implementable and mathematically transparent. The present framework could therefore serve as a classical certified benchmark for future comparisons with quantum or hybrid quantum-classical solvers.

8. Conclusion

The CSPA-SFEM method is an innovative numerical algorithm developed for use in solving Non-Local Quantum Fractional PDEs having variable coefficients by overcoming the major difficulties associated with the computation of numerical solutions to equations containing fractional and non-local operators, whilst allowing the use of natural and simple operator function meshes (i.e., two-dimensional polygons, three-dimensional tetrahedra) onto which fractional or non-local differential operators can be implemented. The CSPA-SFEM methodology provides high accuracy for computing solutions of non-local and fractional hyperbolic PDE problems by combining the spatially dense data operator structures that result from solving the original PDE of the problem under both implicit and explicit conditions and solving for the eigenvalues (determined from boundary value problems) of each operator in the spatial direction using a dual-pronged approach: First, by solving for the "coarse" solution in the traditional spectral approximation approach using global and local FEMs; Second, by using adaptive mesh refinement in conjunction with spectral quality enhancement to supply the necessary local mesh refinement needed in the spectral solutions to accurately approximate the discrete solution of the governing system according to the governing spatial, temporal, coefficient, quadrature, and non-local kernel boundaries would be determined; thereby providing a certified mechanism by which to achieve a higher degree of assurance regarding the numerical quality of the computed solution. In support of the application of CSPA-SFEM for accurately calculating the solutions of long-term simulations of quantum-type systems, numerical simulations demonstrate the use of CSPA-SFEM to provide stable and accurate solutions with good accounting for the fundamental physical characteristics of the governing system of equations. In addition, results show that both the average conservation laws (mass and energ y conservation) associated with two- and three-dimensional CSPA-SFEM simulations demonstrate that negligible drift in the mass or Hamiltonian energy arises during the course of the simulations. These results are very important to provide reliable numerical solutions to problems that exhibit long time histories where man-made or artificial dissipation of energy or numerical accumulation of energy at the boundary conditions would lead to unphysical or unreliable problem results.

References

1. Ainsworth M, Glusa C. Aspects of an adaptive finite element method for the fractional Laplacian: a priori and a posteriori error estimates, efficient implementation and multigrid solver. *Comput Methods Appl Mech Eng*. 2017. https://doi.org/10.1016/j.cma.2017.08.019
2. Atman KG, Şirin H. Nonlocal phenomena in quantum mechanics with fractional calculus. *Rep Math Phys*.

2020. https://doi.org/10.1016/S0034-4877(20)30075-6
3. Azghay A, Massar M, El Mhouti A. Existence and uniqueness results for solutions to fractional p(·,·)-Laplacian problems with a variable-order derivative. *J Nonlinear Model Anal*. 2025. https://doi.org/10.12150/jnma.2025.1482
4. Binev P, Dahmen W, DeVore R. Adaptive finite element methods with convergence rates. *Numer Math*. 2004. https://doi.org/10.1007/s00211-003-0492-7
5. Bringmann P, Miraçi A, Praetorius D. Iterative solvers in adaptive FEM: adaptivity yields quasi-optimal computational runtime. *Adv Appl Mech*. 2024. https://doi.org/10.1016/bs.aams.2024.08.002
6. Bringmann P, Feischl M, Miraçi A, Streitberger J. On full linear convergence and optimal complexity of adaptive FEM with inexact solver. *Comput Math Appl*. 2025. https://doi.org/10.1016/j.camwa.2024.12.013
7. Bulle R, Barrera O, Bordas SPA, Hale JS. An a posteriori error estimator for the spectral fractional power of the Laplacian. *Comput Methods Appl Mech Eng*. 2023. https://doi.org/10.1016/j.cma.2023.115943
8. Cao J, Wang W, Xiao A. Adaptive fast L1–2 scheme for solving time fractional parabolic problems. *Comput Math Appl*. 2025. https://doi.org/10.1016/j.camwa.2024.12.003
9. Chou T, Shao S, Xia M. Adaptive Hermite spectral methods in unbounded domains. *Appl Numer Math*. 2023. https://doi.org/10.1016/j.apnum.2022.09.003
10. Dörfler W. A convergent adaptive algorithm for Poisson's equation. *SIAM J Numer Anal*. 1996. https://doi.org/10.1137/0733054
11. Du Q, Tian L, Zhao X. A convergent adaptive finite element algorithm for nonlocal diffusion and peridynamic models. *SIAM J Numer Anal*. 2013. https://doi.org/10.1137/120871638
12. Feng H, Mavriplis C. Adaptive spectral element simulations of thin premixed flame sheet deformations. *J Sci Comput*. 2002. https://doi.org/10.1023/A:1015137722700
13. Giani S, Graham IG. A convergent adaptive method for elliptic eigenvalue problems. *SIAM J Numer Anal*. 2009. https://doi.org/10.1137/070697264
14. Godinho CFDL, Vancea IV. Fractional calculus in physics: a brief review of fundamental formalisms. *Mathematics*. 2025. https://doi.org/10.3390/math13223643
15. Hafeez MB, Krawczuk M. Fractional spectral and fractional finite element methods: a comprehensive review and future prospects. *Arch Comput Methods Eng*. 2024. https://doi.org/10.1007/s11831-024-10083-w
16. Hendy AS, Zaky MA. Global consistency analysis of L1-Galerkin spectral schemes for coupled nonlinear space-time fractional Schrödinger equations. *Appl Numer Math*. 2020. https://doi.org/10.1016/j.apnum.2020.05.002
17. Hesthaven JS. Spectral penalty methods. *Appl Numer Math*. 2000. https://doi.org/10.1016/S0168-9274(99)00068-9
18. Khalil H, Khan RA, Baleanu D, Rashidi MM. Some new operational matrices and its application to fractional order Poisson equations with integral type boundary constrains. *Comput Math Appl*. 2019. https://doi.org/10.1016/j.camwa.2016.04.014
19. Khalil H, Hashim I, Khan WA, Ghaffari A. A novel method for solution of fractional order two-dimensional nonlocal heat conduction phenomena. *Math Probl Eng*. 2021. https://doi.org/10.1155/2021/1067582
20. Kharazmi E, Zayernouri M, Karniadakis GE. Petrov–Galerkin and spectral collocation methods for distributed order differential equations. *SIAM J Sci Comput*. 2017. https://doi.org/10.1137/16M1073121
21. Kheybari S. Numerical algorithm to Caputo type time–space fractional partial differential equations with variable coefficients. *Math Comput Simul*. 2021. https://doi.org/10.1016/j.matcom.2020.10.018
22. Mavriplis C. Adaptive mesh strategies for the spectral element method. *Comput Methods Appl Mech Eng*. 1994. https://doi.org/10.1016/S0045-7825(94)80010-3
23. Mostafanejad M. Fractional paradigms in quantum chemistry. *Int J Quantum Chem*. 2021. https://doi.org/10.1002/qua.26762
24. Motamarri P, Nowak MR, Leiter K, Gavini V. Higher-order adaptive finite-element methods for Kohn–Sham density functional theory. *J Comput Phys*. 2013. https://doi.org/10.1016/j.jcp.2013.06.042
25. Nguyen T. Quantum algorithms for partial differential equations: a performance review and future trajectories. *Lect Notes Netw Syst*. 2025. https://doi.org/10.1007/978-3-032-11524-9_2
26. Sarma A, Watts TW, Moosa M, McMahon PL. Quantum variational solving of nonlinear and multidimensional partial differential equations. *Phys Rev A*. 2024. https://doi.org/10.1103/PhysRevA.109.062616
27. Song Z, Jung JH. The exact formula of the optimal penalty parameter value of the spectral penalty method for differential equations. *Appl Math Comput*. 2020. https://doi.org/10.1016/j.amc.2020.125313
28. Stevenson R. Optimality of a standard adaptive finite element method. *Found Comput Math*. 2007. https://doi.org/10.1007/s10208-005-0183-0
29. Sun P, Russell RD, Xu J. A new adaptive local mesh refinement algorithm and its application on fourth order thin film flow problem. *J Comput Phys*. 2007. https://doi.org/10.1016/j.jcp.2006.11.005
30. Tang T, Yuan H, Zhou T. Hermite spectral collocation methods for fractional PDEs in unbounded domains. *Commun Comput Phys*. 2018. https://doi.org/10.4208/CICP.2018.HH80.12
31. Tang T, Wang LL, Yuan H, Zhou T. Rational spectral methods for PDEs involving fractional Laplacian in unbounded domains. *SIAM J Sci Comput*. 2020. https://doi.org/10.1137/19M1244299
32. Valenciano J, Owens RG. h–p adaptive spectral element method for Stokes flow. *Appl Numer Math*. 2000. https://doi.org/10.1016/S0168-9274(99)00103-8
33. Xiang M, Hu D, Zhang B, Wang Y. Multiplicity of solutions for variable-order fractional Kirchhoff equations with nonstandard growth. *J Math Anal Appl*. 2021. https://doi.org/10.1016/j.jmaa.2020.124269
34. Xu H, Cantwell CD, Monteserin C, Sherwin SJ. Spectral/hp element methods: recent developments, applications, and perspectives. *J Hydrodyn*. 2018. https://doi.org/10.1007/s42241-018-0001-1

35. Zayernouri M, Karniadakis GE. Fractional spectral collocation methods for linear and nonlinear variable order FPDEs. *J Comput Phys*. 2014. https://doi.org/10.1016/j.jcp.2014.12.001
36. Zhan H, Wang T, Hu G. An unconditionally energy-stable and orthonormality-preserving scheme for the Kohn–Sham gradient flow based model based on a tetrahedral spectral element method. *Commun Comput Phys*. 2025. https://doi.org/10.4208/cicp.OA-2024-0053
37. Zhao T, Mao Z, Karniadakis GE. Multi-domain spectral collocation method for variable-order nonlinear fractional differential equations. *Comput Methods Appl Mech Eng*. 2019. https://doi.org/10.1016/j.cma.2019.01.040

How to Cite This Article
Al-Taie NAAA. Certified Structure-Preserving Adaptive Spectral–Finite Element Method for Nonlocal Quantum–Fractional PDEs with Variable Coefficients. International Journal of Advanced Mathematics and Numerical Research. 2026;2(4):09–23.
doi: https://doi.org/10.54660/IJAMNR.2026.2.4.09-23